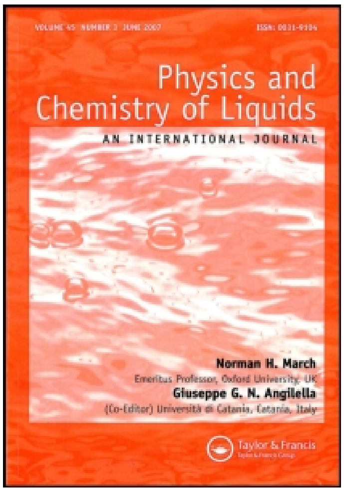

Physics and Chemistry of Liquids
Publication details, including instructions for authors and subscription information:
http://www.informaworld.com/smpp/title~content=t713646857

Thermodynamics and structure of charged hard-sphere fluids in the mean spherical model

M. C. Abramo[a]; C. Caccamo[a]; G. Pizzimenti[a]
[a] Istituto di Fisica dell Universita, Messina, Italy

To cite this Article Abramo, M. C. , Caccamo, C. and Pizzimenti, G.(1977) 'Thermodynamics and structure of charged hard-sphere fluids in the mean spherical model', Physics and Chemistry of Liquids, 6: 3, 167 — 188

To link to this Article: DOI: 10.1080/00319107708084138

URL: http://dx.doi.org/10.1080/00319107708084138

Phys. Chem. Liq., 1977, Vol. 6, pp. 167–188

Printed in Great Britain

Thermodynamics and Structure of Charged Hard-Sphere Fluids in the Mean Spherical Model†

M. C. ABRAMO, C. CACCAMO, and G. PIZZIMENTI
Istituto di Fisica dell 'Universita', Messina, Italy

(*Received December 17, 1976*)

The "mean spherical model" (MSM) for an MX-type fluid of charged hard-spheres of different diameters has been solved numerically. The solution method is discussed in detail. The model allows one to examine thermodynamic and structural properties of charged hard-sphere fluids in a wide range of density and temperature and over the whole range of radius ratio. Internal energies and state equations are discussed while a broad picture of the structure is given through extensive results for the pair correlation function. The partial structure factors for which the model provides analytic expressions, are compared with available experimental and computer simulation data for molten sodium and potassium chloride. The agreement obtained is generally encouraging and almost quantitative when the ionic radii are chosen by fitting the experimental compressiblities.

I INTRODUCTION

Detailed information on the structure of several ionic liquids such as molten sodium and potassium chloride has been obtained in recent years both by neutron diffraction[1–3] and by computer simulation experiments;[4–6] the latter also report results for thermodynamic quantities of main interest.

Various authors[7–9] have proposed in the last few years the mean spherical model (MSM) for charged hard spheres fluids as a simple model approach for electrolyte solutions and ionic liquids; however, explicit solutions of the model have been obtained only in particular limits[7–9] and a complete solution has not yet been obtained for arbitrary sizes of the ionic components. Only recently a numerical solution of the model for this general case has been briefly reported (see Ref. 10, hereafter referred to as I).

---

† Work performed under the auspices of the Gruppo Nazionale di Struttura della Materia del Consiglio Nazionale della Ricerche and of the Comitato. Regionale Ricerche Nucleari e Struttura della Materia.

It is the purpose of this work to give a detailed description of the route followed in the numerical solution of the model and report extensive results for thermodynamic quantities, partial structure factors and pair correlation functions of charged hard-spheres fluids, over the whole range of size ratios and over a wide range of densities and temperatures. Secondly a comparison is made between the MSM and the observed properties of molten alkali halides, for both thermodynamics and structure.

Because of the serious approximations involved the MSM results provide indications of general trends rather than quantitative predictions for real systems†. However some features of this model deserve to be stressed;

i) it is possible, with very simple initial assumptions, to have a broad overview of properties of charged hard sphere fluids and of systems that they could approximate;

ii) the model results can be useful as initial input for more refined theories (YNC) or computer experiments;

iii) the partial structure factors are directly related to the solution of the model itself and once this is known the calculation of the partial structure factors is a simple task. This seems of particular interest for molten alkali halides, where the assumption of complete ionicity of the MSM approach is met and comparison with neutron diffraction data[2,3] is immediately possible.

In Section II the basic equation of the model and the explicit form of the direct correlation functions are briefly recalled; the numerical method of solution is also discussed in detail. In Section III results are presented for coefficients of the model of immediate physical meaning and comparison is made with thermodynamic data for real systems; results for the state equations of NaCl and KCl are also given. Finally in Section IV the dependence of the pair correlation functions on the model parameters is discussed, and the partial structure factors and correlation functions for NaCl and KCl are compared with experiments.

II BASIC EQUATIONS AND NUMERICAL SOLUTION

a Mean spherical model

The Waisman and Lebowitz[7] MSM results for the direct correlation functions $c_{ij}(r)$ for an MX-type ionic liquid are summarized as follows:

---

† For improvements of the original MSM approach see Reference 11 and references given therein.

$$
\begin{aligned}
-c_{ii}(r) &= \left(a_i - \frac{\pi\beta}{3\eta_i} V_{ii}\right) + \frac{M_{ii}}{12\eta_i} r + \frac{1}{2}(\eta_1 a_1 + \eta_i a_2) r^3 && r < \sigma_i \\
&= \frac{\beta e_i^2}{\varepsilon r} && r > \sigma_i
\end{aligned}
\tag{1}
$$

$$
\begin{aligned}
-c_{21}(r) = -c_{21}(r) &= a_1 + \frac{\pi\beta V_{22}}{3\eta_1} && r \leq \lambda \\
&= a_1 + \frac{\pi\beta V_{22}}{3\eta_1} + \frac{M_{21}}{12(\eta_1\eta_2)^{1/2}} \frac{(r-\lambda)^2}{r} && \lambda < r < R \\
&\quad + 2\lambda(\eta_1 a_1 + \eta_2 a_2)\frac{(r-\lambda)^3}{r} && \\
&\quad + \frac{1}{2}(\eta_1 a_1 + \eta_2 a_2)\frac{(r-\lambda)^2}{r} && \\
&= \frac{\beta e_1 e_2}{\varepsilon r} && r > R
\end{aligned}
\tag{2}
$$

Here σ_i is the hard sphere diameter in the i-th ionic species ($i = 1, 2$ and $\sigma_1 \leq \sigma_2$ by convention); $\lambda = \frac{1}{2}(\sigma_2 - \sigma_1)$ and $R = \frac{1}{2}(\sigma_1 + \sigma_2)$; $\eta_i = \pi/6\rho_i$ where ρ_i is the number density of the i-th component; e_i is the ionic charge; $\beta = (k_B T)^{-1}$ and $a_1, a_2, M_{11}, M_{22}, M_{21}, V_{11}, V_{22}$ are a set of seven unknown coefficients whose dependence on physical parameters describing the system such as density, temperature and ionic sizes, has to be determined. V_{11} and V_{22} are defined through:

$$V_{ij} = \frac{72}{\pi}(\eta_i\eta_j)^{1/2} e_j \sum_l \eta_l e_l \int_{\sigma_{il}}^{\infty} x g_{il}(x) \mathrm{d}x \tag{3}$$

where, for convenience, we have introduced the notations $\sigma_{ll} \equiv \sigma_l, \sigma_{12} \equiv R$; their sum,

$$\varepsilon^{-1} \sum_i V_{ii} = E^{ex} \tag{4}$$

gives the excess internal energy or average potential energy per unit volume with screening effects described by dielectric constant ε. a_1 and a_2 are originally introduced through the relations:

$$a_j = 1 - 24 \sum_l \eta_l \int_0^{\sigma_{lj}} c_{lj}^{(0)}(x) x^2 \,\mathrm{d}x \tag{5}$$

where

$$C_{ij}^{(0)}(r) \equiv c_{ij}(r) + \frac{\beta e_i e_j}{\varepsilon r};$$

their meaning in terms of partial molar volumes has been pointed out elsewhere.[9] It should be noted that Eqs. (5) become two linear equations in the seven unknown coefficients upon use of Eqs. (1)–(2).

As a consequence of the very simple form of the direct correlation functions in this model, the Fourier transforms $c_{ij}(q)$ are obtained through a simple integration. Restults are reported in detail in the Appendix.

The direct correlation functions are in turn related to the partial structure factors $S_{ij}(q)$ through the Pearson–Rushbrooke[12] relations:

$$
\begin{aligned}
S_{ii}(q) &= \frac{1 - c_{\bar{i}\bar{i}}(q)}{(1 - c_{11}(q))(1 - c_{22}(q)) - c_{12}^2(q)} \\
S_{12}(q) &= \frac{c_{12}(q)}{(1 - c_{11}(q))(1 - c_{22}(q)) - c_{12}^2(q)}
\end{aligned}
\tag{6}
$$

The MSM thus gives in a direct manner, upon substitution of (A.1) and (A.2) in (6), the partial structure factors and numerical estimate is possible once the solution for the coefficients is known.

Waisman and Lebowitz[7] have shown that the coefficients of the model are related by a set of seven quadratic equations. Of these, however, only five are independent because of the symmetry of the problem under the interchange $\sigma_1 \leftrightarrow \sigma_2$. The other two equations we need are given by (5), so that we have finally to solve a system of two linear and five quadratic equations.

b Numerical solution

The following dimensionless parameters have been introduced to describe the system: the radius ratio $\alpha = \sigma_1/\sigma_2$; the total packing fraction $\eta = \pi/6\rho_c\sigma_2^3(1 + \alpha^3)$, where ρ_c is the number density of ion pairs; and a parameter $\Gamma = e^2/(K_B T \sigma \varepsilon_2)$ describing the relative strength of the Coulombic interaction with respect to the average kinetic energy per particle. Calculations have been restricted to an MX-type liquid, where $|e_1| = |e_2| = e$. The known solutions,[7,9,13,14] for neutral or charged hard-sphere systems in the MSM, refer to the following limits:

$\alpha = 1,$	$\Gamma = 0$:	neutral one-component liquid (Wertheim 1963)
$0 \le \alpha \le 1,$	$\Gamma = 0$:	neutral hard-spheres of different diameter (Lebowitz 1966)
$\alpha = 1,$	$\Gamma \ge 0$:	charged hard spheres of equal diameter (W. L. 1970)
$\alpha = 0,$	$\Gamma \ge 0$:	charged hard spheres with a vanishingly small diameter for one component (GLTM 1976)

The knowledge of these solutions has in fact been crucial to obtain the present numerical solution of the model for $0 \le \alpha \le 1$ and $T \ge 0$.

The numerical routine used was a CERN library routine[15] which calculates, from the solution corresponding to a particular set of η, Γ and α the solution when one or more of these parameters are charged, provided that the new solution is in the vicinity of the old one. Calculations were therefore performed by starting from a known input solution, i.e. one of the limiting cases listed above. In particular, starting from charged hard spheres of equal diameter ($\alpha = 1$), for some initial values of η and Γ, α was progressively decreased by steps of 0.001, every time taking the calculated solution as a new input.

A CDC 7600 computer was used and the equations were satisfied with a precision of better than 10^{-10}. To check that the solutions so calculated were still physically meaningful, two separate conditions were imposed:

a) at the end of the routine, when the limit $\alpha = 0$ was reached, the solution had to coincide with the results of GLTM (1976);

b) starting from the solution for $\Gamma = 0$ and fixed α (Lebowitz, 1966), and increasing Γ by small steps, cross checking, i.e. identity of solutions, was required for equal η, Γ and α sets.

The (b) criterion was ineffective for small values of α, especially for high packings, when a second solution was obtained. This solution violates the symmetry of the cross correlation functions $C_{12} = C_{21}$. Thus it is possible to discard it on physical grounds.

The range of parameters explored was $0.2 \leq \eta \leq 0.385$, $0 \leq \Gamma \leq 60$ and $0 \leq \alpha \leq 1$. Special calculations were carried out in correspondence with estimated values of the parameters for NaCl and KCl. Detailed tables of the values of the model coefficients are collected in Ref. (22). In the following only coefficients with a direct physical meaning will be discussed.

III THERMODYNAMICS

It is known[9] that a_1 and a_2 are related to the partial molar volumes per particles

$$\bar{v}_j = \frac{1}{V}\left(\frac{\partial V}{\partial \rho_j}\right)_{\rho_i} \tag{7}$$

through the simple relation

$$a_j = \beta \frac{\bar{v}_j}{K_T} \tag{8}$$

where K_T is the isothermal compressibility. On the other hand the following exact limit is obeyed by the static structure factor at $q = 0$:[16]

$$\lim_{q \to 0} S_{ij}(q) = S_0 = \rho_c K_B T K_T \tag{9}$$

Making use of $\rho_1\bar{v}_1 + \rho_2\bar{v}_2 = \rho_c(\bar{v}_1 + \bar{v}_2) = 1$ and of (8) and (9) we obtain

$$S_0 = (a_1 + a_2)^{-1} \tag{10}$$

This result could also be obtained through long-wavelength expressions for the $S_{ij}(q)$ reported elsewhere[17] and the use of thermodynamic relations for the two-component systems.[18]

Equation (10) allows a direct comparison of MSM results with experimental K_T or S_0 of real systems. A similar result holds for monoatomic liquids[19] in the PY approximation.

In Figure 1, a_1 and a_2 are plotted for three values of η and two values of Γ, in the range $0 \leq \alpha \leq 1$. At $\alpha = 1$, $a_1 = a_2$ and both quantities are independent of Γ a result already known.[8] At sufficiently low η and α, the model yields $a_2 < 0$, namely, according to (7) and (8), a reduction in the total volume when particles of type 2 are added to the system. Such a behaviour is clearly opposed by increasing temperature (decreasing Γ) and occupied volume (increasing η). This tendency of the system to compact seems a consequence of the Coulombic attraction between unlike particles, whose distance of closest approach decreases with α.

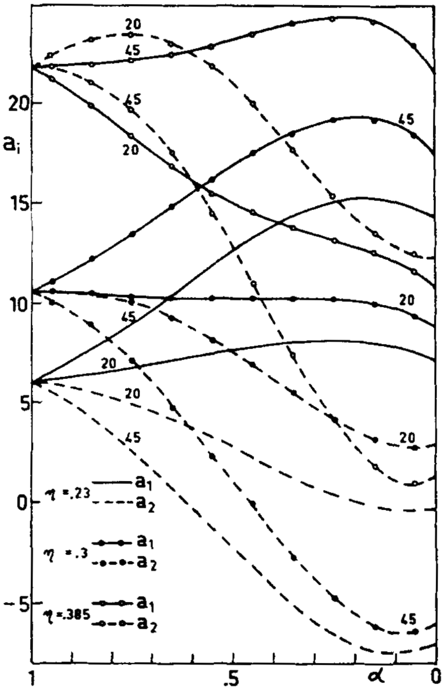

FIGURE 1 a_1 and a_2 vs. α at $\eta = 0.23$, $\eta = 0.3$, $\eta = 0.385$. Labels on the curves are Γ values.

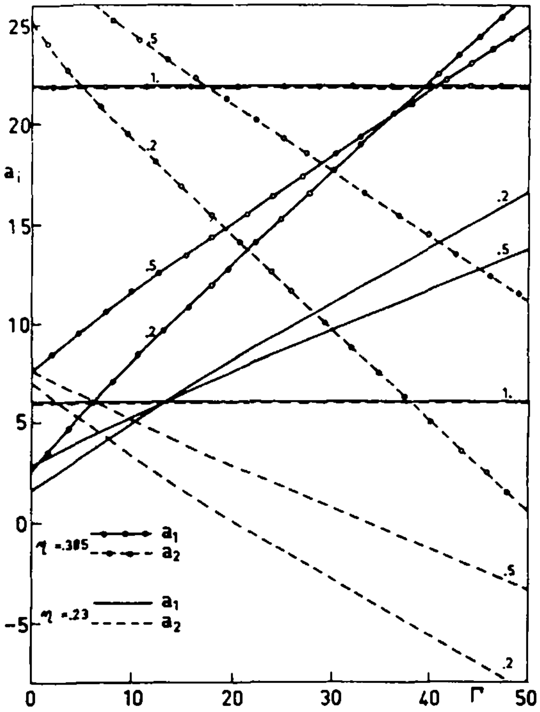

FIGURE 2 a_1 and a_2 vs. Γ at $\eta = 0.23$ and $\eta = 0.385$. Labels are α values.

In Figure 2, a_1 and a_2 are given vs. Γ. As a result of the behaviour of the partial volumes illustrated in this figure, S_0 is practically independent of Γ, particularly for $\alpha > 0.6$. The values of S_0 reported in Table I are representative of a wide range of $\Gamma (20 \lesssim \Gamma \lesssim 60)$.

V_{11} and V_{22} are defined through (3), which we rewrite in a slightly modified form:

$$V_{ii} = 2\pi\rho_i e_i \left[\rho_1 e_1 \int_{\sigma_{i1}}^{\infty} x g_{i1}(x) \mathrm{d}x + \rho_2 e_2 \int_{\sigma_{i2}}^{\infty} x g_{i2}(x) \mathrm{d}x \right]$$

They give the potential energies of particles of types 1 and 2 respectively, in the field of all the others. V_{11} and V_{22} behave quite differently at low α, as shown in Figures 3 and 4. V_{11} begins to increase very steeply while V_{22} is almost flat. This different behaviour is probably related to the behaviour of the like-ions correlation functions at small values of α ($\alpha \leq 0.5$), that we shall discuss in the following. In particular, at these radius ratios, there begins to appear a loss of short range order in the smaller component.

Finally we turn to a comparison with thermodynamic properties of molten NaCl and KCl. MC calculations and computer simulation experiments[5–6]

TABLE I

S_0 values as a function of the packing fraction in the range $\Gamma = 20 \div 60$ and for α values typical of NaCl and KCl.

η	$\alpha = 0.738$	$\alpha = 0.923$
0.23	0.085	0.083
0.25	0.073	0.070
0.30	0.049	0.047
0.36	0.030	0.028
0.385	0.024	0.023

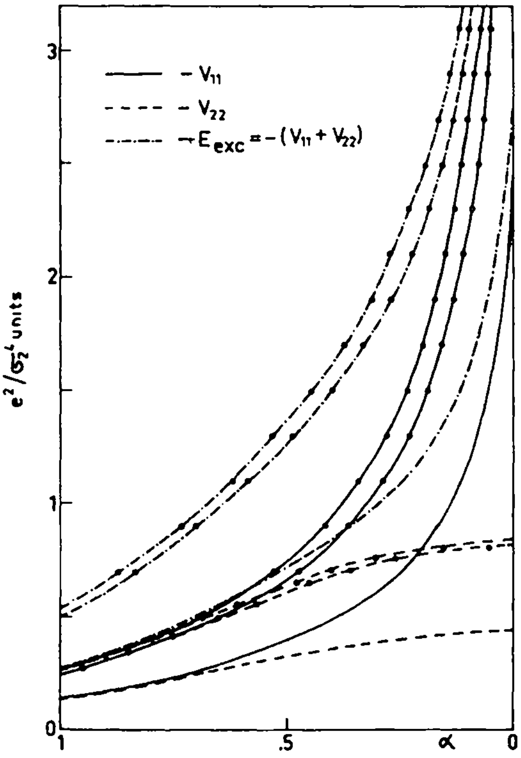

FIGURE 3 V_{11}, V_{22} and E^{ex} vs. α in $e^2/\epsilon\sigma_2^4$ units $\eta = 0.23$, $\Gamma = 20$ unlabelled curves; $\eta = 0.385$, $\eta = 20$, $\eta = 385$, $\Gamma = 45$.

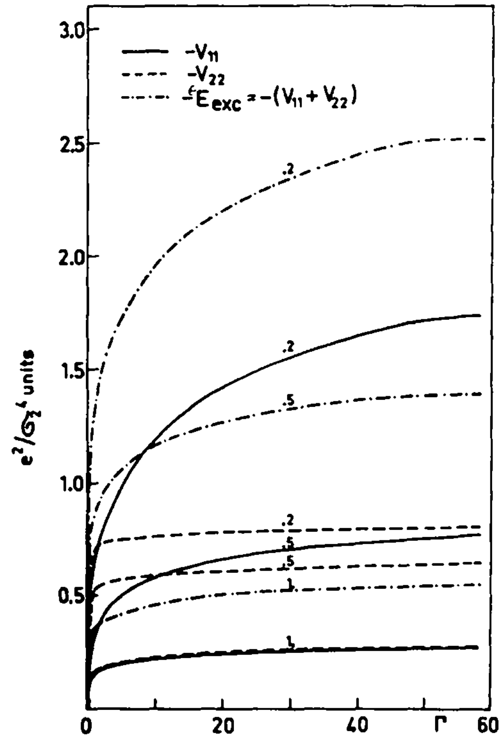

FIGURE 4 V_{11}, V_{22} and E^{ex} vs. Γ, $e^2/\varepsilon\sigma_2^4$ units at $\eta = 0.385$. Labels are α values.

for these molten salts using the Tosi–Fumi potential[20] have given quite satisfactory results so that we have performed a first calculation assuming as radii for our hard-sphere model the crystalline soft-core radii of the ions of the Tosi–Fumi theory. In particular we have assumed $\sigma_{Cl} = 3.17$ Å and $\sigma_{Na} = 2.358$ Å, so that $\alpha = \sigma_+/\sigma_- = .738$ for sodium chloride; $\sigma_{Cl} = 3.17$ Å, $\sigma_K = 2.926$ Å and $\alpha = 0.923$ for potassium chloride. η and Γ are calculated by specifying $\rho_c(T)$.[21] The dielectric constant appearing in the expression of Γ may be put equal to 1, but in a comparison with experimental data lower values could be allowed and interpreted as a consequence of $\varepsilon > 1$. We actually report results for various Γ values, corresponding to $\varepsilon = 1 \div 1.2$.

The results for S_0 do not reproduce the experimental values obtained through (10) e.g. for NaCl at 1073 °K we have $S_0^{exp} = 0.068$ while $S_0^{MSM} = 0.026$. The agreement cannot be improved with variations in Γ, since as noted above S_0 is largely independent of Γ in the model.

The internal energies U are reported in Table II and compared with experimental or computer simulation data. Energies are underestimated

TABLE II

Internal energies for NaCl and KCl, at various temperatures. Values marked with an asterisk correspond to $\varepsilon = 1.2$.

	T(°K)	σ_{Cl}	η	Γ	U_{MC}(kJ/M)	U_{MSM}(kJ/M)
NaCl ($\alpha = 0.738$)	1073	3.17	0.375	49.08	-691.9^a	−731.5
		2.801	0.259	46.3*		−667.05
	1164.5	3.17	0.364	45.22	-686.0^b	−716.5
		2.736	0.234	43.67*		−665.1
KCl ($\alpha = 0.923$)	1045	3.17	0.367	50.4	-625.5^c	−646.3
		2.825	0.260	47.11*		−582.4

[a] Lawis and Singer (1975);
[b] Lantelme *et al.* (1974);
[c] Woodcock and Singer (1971).

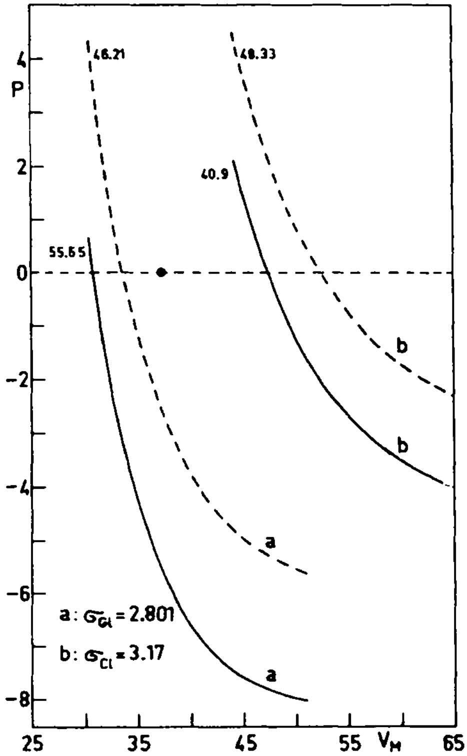

FIGURE 5 State equations for KCl with two values of σ_{Cl} and various Γ. Experimental molar volume of NaCl.

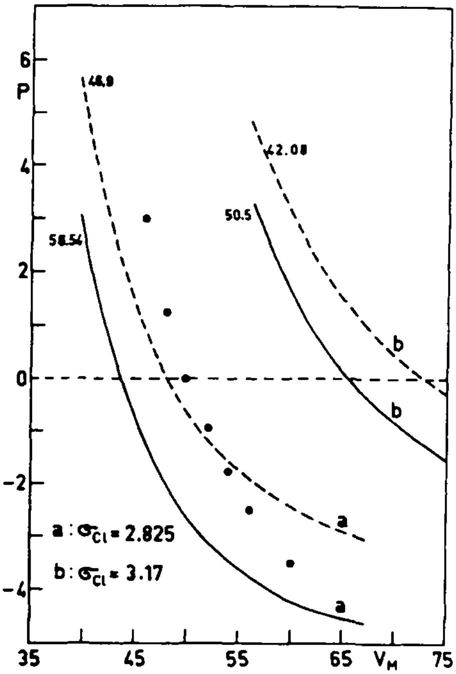

FIGURE 6 State equation for KCl with two values of σ_{Cl} and various Γ. Computer simulation results (Woodcock–Singer) for NaCl at 1045.

though not far from the true value and the agreement improves upon decreasing Γ. Finally the state equations have been considered and pV isotherms compared in Figure 5 and Figure 6 with available data at two Γ values. The MSM curves are located considerably above the data and the molar volume at zero pressure is overestimated.

Some remarks on the use of crystalline radii should be made at this point. There is reason *in principle* that the model hard-core radii should be smaller than crystalline radii, since the latter are fixed so that their sum agrees with the lattice constant, i.e. with the minimum of the cohesive energy, whereas a value of σ_{12} closer to the zero of the unlike-ion potential would be more appropriate for use in a rigid-sphere model such as the present one. Furthermore, with increasing kinetic energy (the temperature is that of a molten salt) the particles test more and more internal regions of the short range repulsive part of the crystalline potential. Temperature dependent ionic radii could then be considered and their value determined by fitting some thermodynamic property. A similar procedure has already been used elsewhere to adjust hard-sphere structure factors for monoatomic liquids to experiments.[19]

Calculations have thus been repeated for the same α values in order to preserve at best the features of the Tosi-Fumi potential, but determining the radii so as to fit the calculated S_0 to the measured ρ_c and K_T.[21] This task is facilitated and the fitting unique because S_0 is, for a given α, only a function of η, as noted above. The new value of σ_{Cl} is easily obtained from the η which corresponds to the fit.

Table II and Figures 5 and 6 show results for the reduced radii: in the range of Γ values considered the internal energies still agree within $\pm 5\,\%$ with the experimental results, while there is a definite improvement for the pV isotherms. A proper choice of Γ could also give the correct value for the molar volumes at zero pressure in both NaCl and KCl. Different results for compressibilities when calculated from pV curves, or through (10) used above to fit experimental values, are a consequence of the well known lack of thermodynamic consistency of the MSM, recently removed in the framework of GMSA (generalized mean spherical approximation)[11] for spheres of equal diameters.

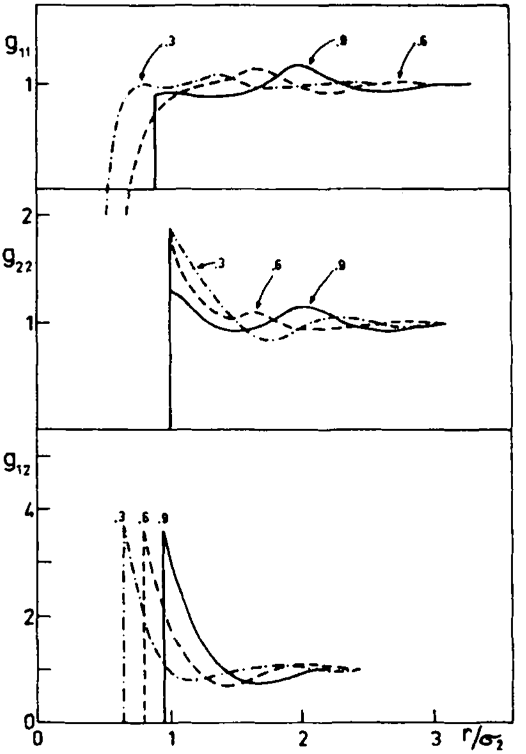

FIGURE 7 $g_{ij}(r)$ vs. $r' = r/\sigma_2$ at $\eta = 0.3$, $\Gamma = 7.2$. Labels are α values.

IV STRUCTURAL PROPERTIES

a Behaviour of pair correlation functions

Results for the general behaviour of pair correlation functions relative to variations of η, Γ and α are presented in Figures 7, 8 and 9, while comparison with experimental data for some alkali halides will be made in the second part of this section.

Two packings, i.e. $\eta = 0.3$ and $\eta = 0.36$ and two Γ values, i.e. $\Gamma = 7.2$ and $\Gamma = 45.4$ are considered with $0 \leq \alpha \leq 1$; similar information at lower can be obtained from Figures 13 and 14.

By comparing Figure 7 and Figure 8 we note that peaks in the g's and oscillations at large r increase in magnitude when Γ is increased, whereas they are much less sensitive to variations in η (cfr. Figures 8 and 9). The same is true for the contact value of g_{12}, which is almost doubled when passing from $\Gamma = 7.2$ to $\Gamma = 45.4$.

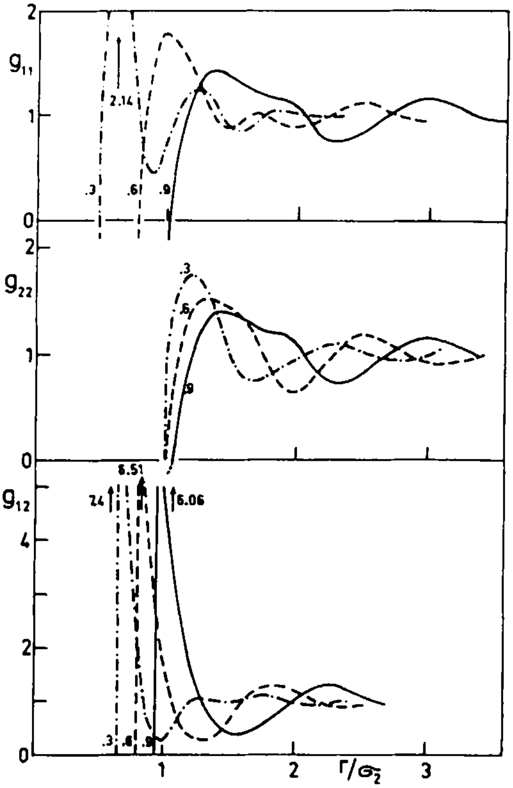

FIGURE 8 $g_{ij}(r)$ vs. $r' = r/\sigma_2$ at $\eta = 0.3$, $\Gamma = 45.4$. Labels are α.

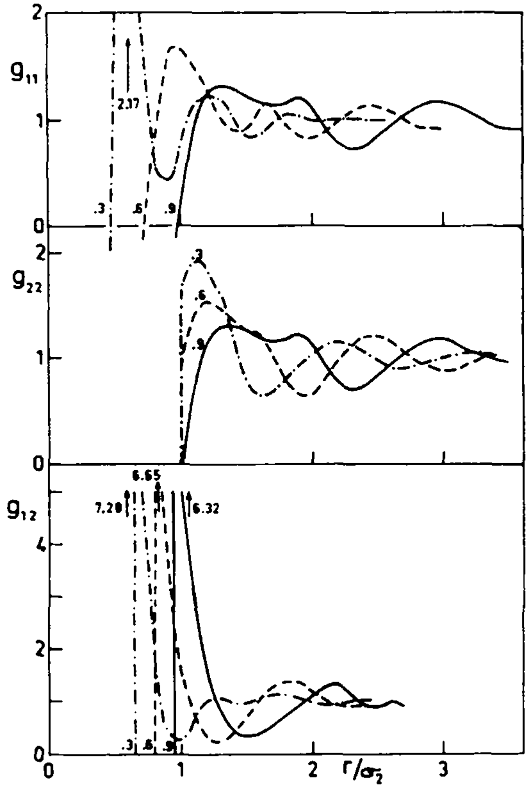

FIGURE 9 $g_{ij}(r)$ vs. $r' = r/\sigma_2$ at $\eta = 0.36$, $\Gamma = 45.4$. Labels are α.

This assigns a major role in determining the structure to the relative strength of the interaction more than to packing effects, at least for $0.23 \leq \eta \leq 0.36$. The dependence of structural features on α is characterized, at high Γ, by the enhancement of the main peak in g_{11} and g_{22} and by its shift towards low r, when α is lowered. Furthermore there is a rapid damping of oscillations of g_{11} and g_{12} at large r when $\alpha \simeq 0.3$, while g_{22} is still oscillating considerably.

As already noted in I, when the same discussion was made in terms of structure factors, the shape of g_{11} suggests that there is appreciable order in this component beyond the first like coordination shell, as long as we consider the intermediate or high α region ($\alpha > 0.5$). When α is further lowered there is a rapid loss of order for component 1.

For some values of the parameters (as indicated in the figures) the pair correlation functions for like ions become negative at small r, this feature being, of course, a direct consequence of the MSM approximation.

The general appearance of these results is in agreement with results of computer simulation experiments for systems of varying relative sizes of the components, such as NaCl,[5] KCl,[4] LiCl[6] and LiI.[6] In particular, they confirm the shift in the peaks and their narrowing and increasing with decreasing α, and the stronger oscillations in the g's at large r.

b Detailed comparison with measured structure factors

NaCl–Neutron diffraction results have been reported for this salt at 1148 °K by Enderby *et al.*[3] and a first comparison with MSM structure factors, calculated through (4–6) was made for η, Γ and α obtained with $\sigma_{Cl} = 3.17$ Å (soft core spheres). Here and in the following $\varepsilon = 1$. Results are given in Figure 10. The agreement, especially in the low q region, is qualitative and only gross features of the measured structure factors are reproduced. Results seem somehow to improve with increasing q.

Calculations were repeated for reduced radii, taking $\sigma_{Cl} \cong 2.8$ Å and the same radius-ratio α, as by the fit of the experimental S_0 discussed above in

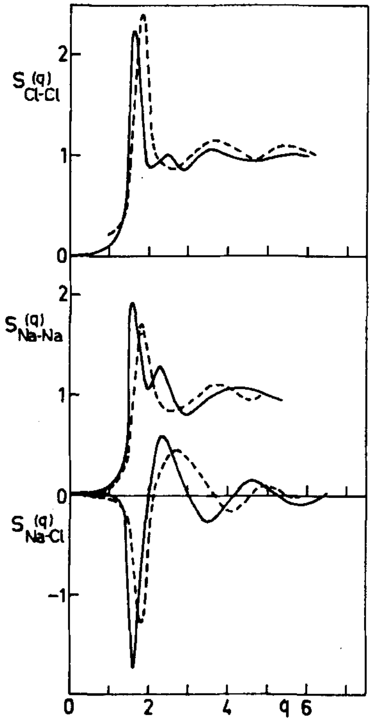

FIGURE 10 $S_{ij}(q)$ vs. q with $\sigma_{Cl} = 3.17$ for NaCl at 1148°K. Full line MSM results, dashed line neutron diffraction experiment.[3] Bars give experimental uncertainties.

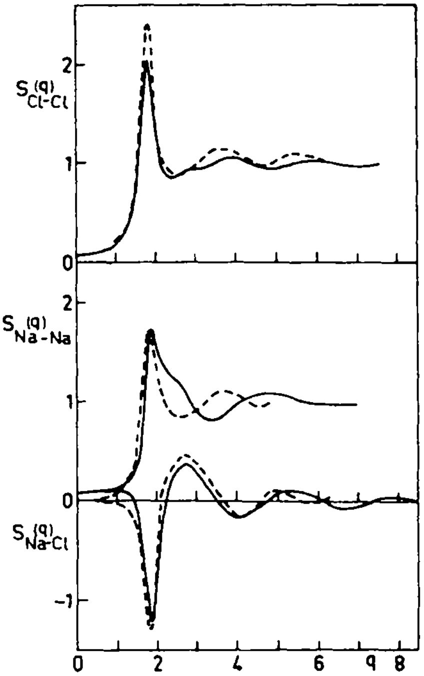

FIGURE 11 $S_{ij}(q)$ vs. q with $\sigma_{Cl} = 2.75$ for NaCl at 1148°K. Full line MSM results, dashed line neutron diffraction experiment.[3] Bars give experimental uncertainties.

Section III. The results are given in Figure 11. There is now almost quantitative agreement with experiment, except in the high q region where results are getting worse especially for S_{12}. The latter feature is probably a consequence of the hard-core representation of the interionic potential.

Not reported in Figures 10 and 11, the height of the peaks decreases with decreasing Γ.

KCl-comparison is made with neutron diffraction data of Derrien and Dupuy[2] using reduced radii; again the low q region is well reproduced (Figure 12).

It clearly appears from these results that when the $q = 0$ limit of is exactly reproduced through a reduction in the soft-core radii, as suggested by general arguments, substantial improvements occur on a wide range of q values for both position and height of main peaks and successive minimum.

c Pair correlation functions for NaCl and KCl

In Table III the main features of calculated and experimental pair correlation functions for NaCl and KCl are reported, while the full shape of $g_{ij}(r)$, as

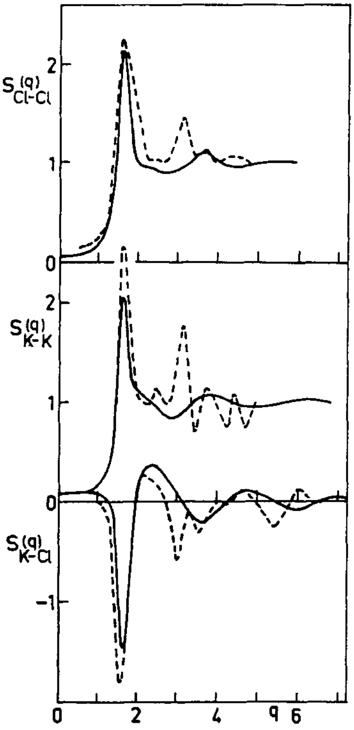

FIGURE 12 $S_{ij}(q)$ vs. q with $\sigma_{Cl} = 2.806$ for NaCl at 1073°K. Full line MSM results, dashed line neutron diffraction.[2]

obtained for NaCl at 1148 °K and KCl at 1073 °K, are shown in Figures 13 and 14 respectively. The reduced radii results (illustrated in these figures) are closer to the experiments almost everywhere. However there is some underestimate of the coordination number when reduced diameters are used. This quantity, defined through the general expression for like and unlike neighbours $n_{\alpha\beta}(r) = 4\pi\rho_c \int_0^r dr' r'^2 g_{\alpha\beta}(r')$, turns out to be 4.5 ÷ 5 in NaCl when $\sigma_{Cl} = 2.8$ Å and 5.8 ± 0.1 when $\sigma_{Cl} = 3.17$ Å, against an experimental value 5.8 ÷ 5.9, and a value of 5.2 according to MC calculations.[6]

The pair, function g_{12} is almost insensitive, both in the contact value and in its general form, to variations of σ_{Cl} (or of the packing), the cutoff position only being varied. Thus, the probability distribution of unlike ions immediately around a given ion is essentially unaltered, but the available volume is drastically reduced when the radii are lowered, thus depressing coordination. Although results at very small distance (and correspondingly at high q's, as noted above) seem to worsen on decreasing the radii, there is an improvement in the model predictions on a larger distance scale, as also

TABLE III

Features of $g_{ij}(r)$ for NaCl and KCl at various temperatures. r_{max} and h are the position and height of the first maximum, respectively; r_{min} the position of the first minimum; n is the coordination number.

				g_{++}				g_{--}				g_{+-}			
		$T(°K)$	$\sigma_{Cl}(Å)$	r	h	r_{min}	n	r	h	r_{min}	n	r	h	r_{min}	n
	Edwards *et al.* (1975)	1148		3.7	1.7	6	13±0.5	3.8	1.9	5.8	13±0.5	2.6	3.3	3.8	5.8
	Lewis *et* al. (J. C. S. II, NaCl 71: 301, 1974)	1073	3.17	4.25	–	–	13.9	4.25	–	–	14.7	2.7	–	–	5.2
	MSM	1148	2.75 3.17	3.4 3.6	1.7 1.45	5.6 6.7	10.4 –	3.85 4.1	1.5 1.4	6.04 6.7	13.7 18.3	2.4 2.75	6.7 6.5	3.75 4.3	4.5 5.8
	Derrien *et al.* (75)	1073		4.85	2.3	6.3 ÷7	12.04÷ 15.9	4.82	1.8	6.3 ÷7	12.3÷ 16.2	3.06	3.03	4.85	6.1
KCl	Woodcock *et al.* (71)	1045	3.17	4.3	1.8	6.65	15.7	4.3	1.8	6.65	15.7	2.97	3.74	4.55	5.7
	MSM	1073	2.806 3.17	4 4.43	1.6 1.51	6.52 7.30	12.7 19.6	4.2 4.4	1.55 1.3	6.45 7.3	13.65 19.3	2.69 3.04	6.47 6.47	4.38 4.75	5 5.8

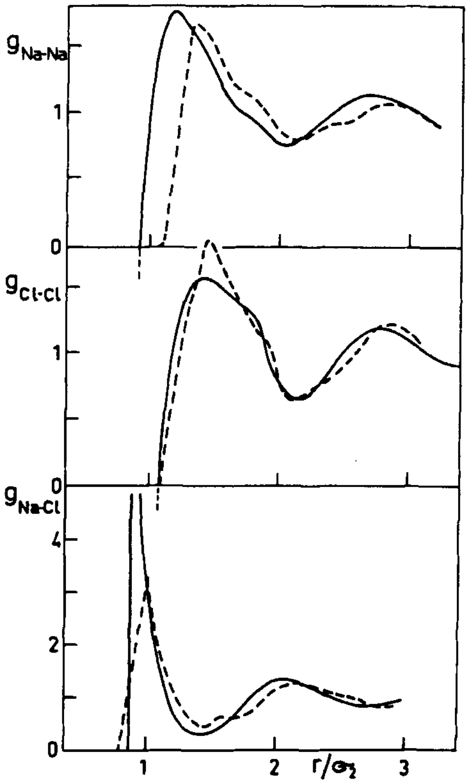

FIGURE 13 $g_{ij}(r)$ vs. r' with $r' = r/\sigma_2$ with $\sigma_2 = 2.75$ for NaCl at 1148°K. Full line MSM results, dashed line Fourier inversion of neutron diffraction experiments.

shown by the like-neighbours coordination number (for instance, $n_{--} \simeq 13.7$ in NaCl against the experimental value 13 ± 0.5 and the simulation result 14.7).

V CONCLUSIONS

The MSM for an MX-type fluid of charged hard spheres of different diameters has been solved numerically. Results are shown for a wide range of possible physical situations and for all values of the radius ratio. A comparison is also made with thermodynamics and structural properties of NaCl and KCl as deduced from experiment and simulation. From a general point of view the model solution allows one to examine how much the structural properties are influenced by variations in the radius ratio (see also I) and by the variations in the interaction strength or the temperature.

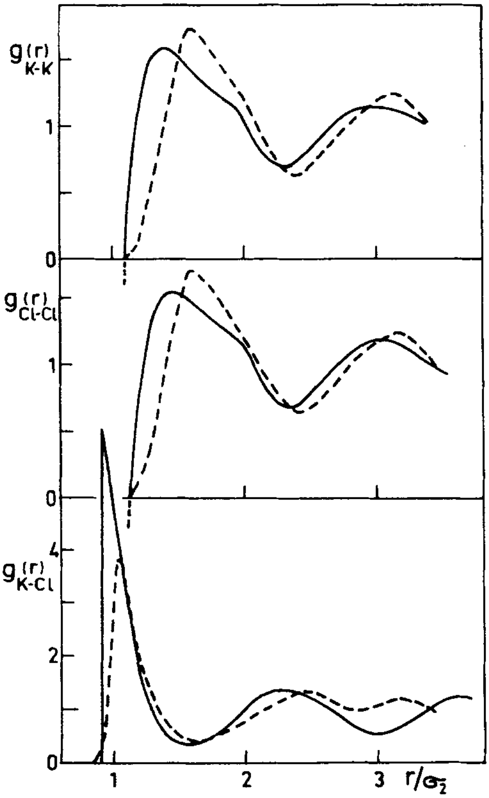

FIGURE 14 $g_{ij}(r)$ vs. r' with $r' = r/\sigma_2$ with $\sigma_2 = 2.806$ for KCl at 1073°K. MSM results full line. Dashed line M.C. calculations for KCl at 1045°K.

More specifically the model predictions based on radius ratios adjusted the thermodynamic liquid-state data, provide an initial knowledge of the gross features of the structure which could be useful as input for more refined theories or for computer experiments.

Acknowledgement

We are grateful to Prof. M. P. Tosi for continuous assistance during this work and for revising the final manuscript, and to Dr. M. Parrinello for many helpful discussions.

Appendix

We report here the detailed expressions for the direct correlation functions in Fourier transform, in terms of the MSM parameters. By Fourier transforming Eqs. (1) and (2), we obtain:

$$c_{ii}(q) = \frac{24\eta_i\sigma_i^3}{(q\sigma_i)^2}\left\{A_i(q)\cos q\sigma_i - B_i(q)\frac{\sin q\sigma_i}{q\sigma_i} + \frac{1}{(q\sigma_i)^2}C_i(q)\right\} \tag{A1}$$

$$c_{12}(q) = \frac{24(\eta_1\eta_2)^{1/2}}{(qR)^2}\left\{A(q)\cos qR - B(q)\frac{\sin qR}{qR}\right. \\ \left. + D(q)\frac{\eta\mu q\lambda}{q\lambda} + E(q)\frac{\cos q\lambda}{(qR)^2}\right. \tag{A2}$$

Here

$$\begin{aligned} A_i(q) &= \left[\alpha_i + b_i + c_i - \frac{\beta l_i^2}{\varepsilon\sigma_i}\right] - \frac{1}{(q\sigma_i)^2}[2b_i + 12c_i] + \frac{24c_i}{(q\sigma_i)^4} \\ B_i(q) &= [\alpha_i + 2b_i + 4c_i] - \frac{24c_i}{(q\sigma_i)^2} \\ C_i(q) &= 2b_i - \frac{24c_i}{(q\sigma_i)^2} \end{aligned} \tag{A3}$$

with

$$\alpha_i = a_i - \frac{\pi\beta V_{ii}}{3\eta_i}, \quad b_i = \frac{M_{ii}\sigma_i}{12\eta_i}, \quad c_i = \frac{\sigma_i^3}{2}(\eta_1 a_1 + \eta_2 a_2) \tag{A4}$$

and also

$$\begin{aligned} A(q) &= \left[\alpha + b + c + d - \frac{\beta e_1 e_2}{\varepsilon R}\right] - \frac{1}{(qR)^2}[2b + 12e] + \frac{24c}{(qR)^4} \\ B(q) &= [\alpha + 2b + 4c] - \frac{24c}{(qR)^2} \\ D(q) &= -\frac{24c\lambda/R}{(qR)^2} \\ E(q) &= \left[2b + 12\left(\frac{\lambda}{R}\right)^2 c\right] - \frac{24c}{(qR)^2} \end{aligned} \tag{A5}$$

with

$$
\begin{aligned}
\alpha &= a_1 + \frac{\pi\beta V_{22}}{3\eta_1} + \frac{\lambda}{6(\eta_1\eta_2)^{1/2}}\left[-M_{21} + 24\lambda_2\sqrt{\eta_1\eta_2}(\eta_1 a_1 + \eta_2 a_2)\right] \\
b &= \frac{R}{12(\eta_1\eta_2)^{1/2}}\left[M_{21} - 36\lambda^2(\eta_1\eta_2)^{1/2}(\eta_1 a_1 + \eta_2 a_2)\right] \\
c &= \frac{R^3}{2}(\eta_1 a_1 + \eta_2 a_2) \\
d &= \frac{\lambda^2/R}{12(\eta_1\eta_2)^{1/2}}\left[M_{21} - 18\lambda^2\sqrt{\eta_1\eta_2}(\eta_1 a_1 + \eta_2 a_2)\right]
\end{aligned}
\tag{A6}
$$

References

1. D. I. Page and K. Mika, *J. Phys. C: Sol. St. Phys.*, **4**, 3034 (1971).
2. J. Y. Derrien and J. Dupuy, *J. Phys. Paris*, **36**, 191 (1975).
3. F. G. Edwards, J. E. Enderby, R. A. Howe, and D. J. Page, *J. Phys. C: Sol. St. Phys.*, **8**, 3483 (1975).
4. L. V. Woodcock and K. Singer, *Trans. Faraday Soc.*, **67**, 12 (1971).
5. F. Lantelme, P. Turq, B. Quentrec, and J. W. E. Lewis, *Mol. Phys.*, **28**, 1537 (1974).
6. J. W. E. Lewis, K. Singer, and L. V. Woodcock, *J. C. S. Faraday II*, **71**, 301 (1975);
   J. W. E. Lewis and K. Singer, *J. C. S. Faraday II*, **71**, 41 (1975);
   M. J. L. Sangster and M. Dixon, *Adv. in Phys.*, **25**, 247 (1976).
7. E. Waisman and J. L. Lebowitz, *J. Chem. Phys.*, **56**, 3086 (1972).
8. E. Waisman and J. L. Lebowitz, *J. Chem. Phys.*, **52**, 4307 (1970).
9. M. Gillan, B. Larsen, M. P. Tosi, and N. H. March, *J. Phys. C: Sol. St. Phys.*, **9**, 889 (1976).
10. M. C. Abramo, C. Caccamo, G. Pizzimenti, M. Parrinello, and M. P. Tosi, *J. Phys. C: Sol. St. Phys.*, **9L** 593 (1976).
11. J. S. Hoye, J. L. Lebowitz, and G. Stell, *J. Chem. Phys.*, **61**, 3253 (1974); G. Stell and S. F. Fun, *J. Chem. Phys.*, **63**, 5333 (1975).
12. F. J. Pearson and G. S. Rushbrooke, *Proc. Roy. Soc.*, **A64**, 305 (1957).
13. J. L. Lebowitz, *Phys. Rev.*, **133**, A895 (1964).
14. H. Wertheim, *Phys. Rev. Lett.*, **8**, 321 (1963).
15. M. Gerard, Cern Computer 6000 Series Progr. Library, C400 (1971).
16. M. C. Abramo, M. Parrinello, and M. P. Tosi, *J. Nonmetals*, **2**, 57 (1973).
17. P. V. Giaquinta, M. Parrinello, and M. P. Tosi, *Phys. Chem. of Liquids* (in press).
18. J. G. Kirkwood and F. Buff, *J. Chem. Phys.*, **19**, 774 (1951).
19. L. Verlet, *Phys. Rev.*, **165**, 201 (1968).
20. M. P. Tosi and F. C. Fumi, *J. Phys. Chem. Solids*, **25**, 31 (1964).
21. G. J. Janz, *Molten salts Handbook*, Academic Press, (New York), 1967.
22. M. C. Abramo, C. Caccamo, and G. Pizzimenti, *Numerical results for MSM in charged hard-spheres fluids.* Internal Report No. 1 (1976) Ist. di Fisica, Univ. Messina.